# Electrochemical, Spectroscopic and Molecular Docking Studies on the Interaction between Human Serum Albumin and Natamycin

# Masoud Fouladgar<sup>1,\*</sup> and Maryam Khademi Dehkordi<sup>1</sup>

Department of Biology, Fal.C., Islamic Azad University, Isfahan, Iran \*Corresponding author: Masoud.Fouladgar@iau.ac.ir

Received 19/05/2025; accepted 12/09/2025 https://doi.org/10.4152/pea.2027450402

#### **Abstract**

Interaction between Human Serum Albumin (HSA) and Natamycin (NA), a widely used antifungal agent, was herein investigated using a combination of electrochemical, spectroscopic and molecular docking (MD) techniques. UV-Vis spectroscopy revealed that interaction between HSA and NA leads to structural changes in HSA, evidenced by increased absorption peaks. Electrochemical studies demonstrated that NA exhibits irreversible oxidation on a glassy carbon electrode, and its electrochemical activity decreases in presence of HSA, indicating complex formation. Thermodynamic analysis suggested that binding process is spontaneous, driven primarily by Van der Waals forces and hydrogen bonds, with a binding constant ( $K_b$ ) of  $6.86 \times 10^3$ , at 298 K. MD further confirmed the interaction, identifying Sudlow site I as primary binding site, with a binding energy of -8.78 kcal/mol.

*Keywords:* human serum albumin; molecular docking; Natamycin; spectroscopy; voltammetry.

## Introduction•

Natamycin (NA), a natural fungicide formerly known as pimaracin or tennectin, was first isolated in 1955 [1-4]. It has a molar mass of 665.725 g/mol, it is amphoteric, and it has an isoelectric point of 6.5 [4, 5]. NA is a polyene macrolide antifungal produced by actinomycete *Streptomyces natalensis* and related species, effective against yeasts and moulds, but ineffective against bacteria [2, 4].

Polyene macrolide antibiotics feature a lactonized ring of carbon atoms that includes a system of conjugated double bonds and a hydrophilic region with hydroxyl groups. They may also possess a glycosidically linked carbohydrate residue and various carboxyl, aliphatic or aromatic groups attached to the ring [6]. NA's primary

<sup>•</sup> The abbreviations and symbols definitions lists are in page 255.

structure features a large lactone ring composed of 25 carbon atoms, linked to a mycosamine moiety, m-amino-sugar, via a glycosidic bond. It is categorized as a tetraene, due to its four conjugated double bonds. Mycosamine portion (3-amino-3,6-dideoxy-D-mannose) at C15 position forms a six-membered pyranose ring. The molecule adopts a cylindrical shape, with hydroxyl groups from its amphipathic chain oriented towards each other, while its exterior remains entirely non-polar. Solubility of NA in water is very low, ranging from 20 to 50 mg/L [5]. NA is used medically to treat fungal infections of the eye, particularly those affecting clear corneal surface, due to its potent inhibitory effects, minimal side effects, lower ocular toxicity and reduced risk of resistance compared to other antifungals [3, 7]. It is also employed to treat other fungal infections in vagina, hair, mucous membranes, nails and skin [5]. NA exhibits antifungal activity against both filamentous and nonfilamentous fungi, including species of Candida, Aspergillus, Fusarium, Microsporum, Trichophyton and Epidermophyton [3, 5]. NA acts by binding to ergosterol in membranes of yeasts and molds, increasing cell's membrane permeability and disrupting plasma membrane transport, ultimately leading to fungal cell death [1, 4, 8]. Systematic use of NA may cause nausea, vomiting and diarrhea as side effects [5].

In food industry, NA is used as antifungal biopreservative additive or edible natural antimicrobials film [2, 4]. Although, application of NA as food preservative is closely monitored due to potential health risks, several countries have approved its application in wine and dairy products [2, 9].

European Food Safety Authority's Panel on Food Additives has determined that children's highest potential exposure to NA is 0.1 mg/kg bw/day. The Panel has concluded that proposed levels of NA are safe when used solely for surface treatment of semihard and semisoft cheese rinds and certain sausage casings [5, 10]. US Food and Drug has stated that NA levels in cheese should not exceed 20 mg/kg in the final product [11].

Human serum albumin (HSA) is the most abundant transport protein in blood, making up over half of serum composition [12, 13]. It is also found in saliva, lymph, interstitial fluid and cerebrospinal fluid [13]. HSA is synthesized in the liver with a half-life of 17 to 19 days. Processes involved in its degradation are not well understood; however, it is believed to primarily take place in skin, muscles, liver and kidneys [12, 14]. HSA is a widely recognized multifunctional protein that serves as carrier for hormones [15], nutrients [16], metabolites [17], metal ions [18], metal nanoparticles [19], fatty acids [20, 21] and drugs [22-24]. Despite its high water solubility, HSA's large molecular size inhibits rapid kidney elimination, making it suitable for drug delivery [14, 22]. HSA consists of a single polypeptide chain organized into three homologous domains— I, II and III—, along with subdomains A and B that form its three-dimensional structure [22, 23]. Two main ligand-binding

sites have been identified: Sudlow site I and Sudlow site II (warfarin and benzodiazepine binding sites) which are located within subdomains IIA and IIIA, respectively [25, 26].

Various experimental methods have been applied for study interaction and binding between HSA and other species. including calorimetry [27], fluorescence [28], 3D fluorescence [28, 29] circular dichroism spectroscopy [28, 20], atomic force microscopy [27], UV-Vis spectroscopy[29,30], resonance light scattering [30], Raman spectroscopy [31], nuclear magnetic resonance spectroscopy [32] and mass spectrometry [33]. Additionally, electrochemical methods have been utilized for this purpose [34, 35]. Despite being simple, fast and low-cost, there are few reports utilizing these methods, to our knowledge. In electrochemical methods it is required that species undergo oxidation or reduction on the electrode surface, to allow investigation of interactions between HSA and redox-active species. In this case, the effect of interaction between HSA and species can be investigated through electrochemical techniques. If the species under investigation is not electroactive or displays weak activity, compounds like potassium ferricyanide, which can be reversibly oxidized and reduced on the electrode surface, may be employed as probes to study albumin's interaction with it [36, 37]. In addition, theoretical and computational methods, including molecular dynamics simulation [38, 39], molecular docking (MD) [38, 40], principal component analysis [19, 28] and free energy landscape analysis [31, 41], have been utilized to characterize the interaction of HSA with other species.

This study first examined the interaction between HSA and NA using UV-Vis spectroscopy and electrochemical techniques, followed by MD, to identify the potential binding site of HSA and NA.

## Materials and methods

## Materials and solutions

HSA and NA were purchased from Sigma-Aldrich. Stock solution of HSA was prepared in a phosphate buffer solution (pH = 7.4, 0.02 mol/L<sup>-1</sup>). Exact concentration of HSA was determined by measurement absorbance at 280 nm, and using Beer-Lambert equation (A=  $\epsilon$ bc,  $\epsilon$  = 36,500 M<sup>-1</sup>/cm<sup>-1</sup>) [40]. Phosphate buffer was prepared by mixing sodium hydrogen phosphate and sodium dihydrogen phosphate, and adjusting pH to 7.4 using a Metrohm pH meter (model 827).

#### Spectroscopic study

To record UV-Vis spectra in the range from 200 to 450 nm, a Shimadzu UV-2100 spectrophotometer was applied. Measurements were taken in quartz cells ( $1 \times 1$  cm), and temperature was adjusted using a thermoelectric temperature controlled cell holder.

## Electrochemical study

All electrochemical measurements were conducted at 25±1 °C using a computerized potentiostat/galvanostat system (SAMA 500, Iran). Measurements were performed in a three-electrode cell assembly comprising a 50 mL glass cell with an Ag/AgCl electrode as reference electrode (RE), a platinum wire counter electrode and a glassy carbon working electrode (geometric area = 0.23 cm²). All potentials were reported relative to Ag/AgCl reference electrode.

## Experimental procedure

To record absorption spectra, 2 mL of  $1.5 \times 10^{-5}$  mol/L<sup>-1</sup> HSA in phosphate buffer (pH = 7.4) were added to the cell. After temperature adjustment, the solution was titrated with  $1.0 \times 10^{-3}$  mol/L<sup>-1</sup> NA. Absorption spectrum was recorded at each step. For electrochemical analysis, 10 mL phosphate buffer were added to the electrochemical cell. Electrochemical measurements were performed after adding appropriate amounts of NA ( $1.0 \times 10^{-3}$  mol/L<sup>-1</sup>) and HSA ( $6.0 \times 10^{-5}$  mol/L<sup>-1</sup>) solutions. Cyclic voltammograms (CV) were recorded for each solution in the potential range from 0.5 to 1.3 V, at a scan rate of 100 m/s<sup>-1</sup>. Chronoamperograms were obtained by applying a potential step of 1.2 V.

# Molecular docking

For docking investigation, RCSB protein data bank has been used to access HSA (PDB ID: 6m4r), and 3D structure of NA as ligand was retrieved from Pubchem with CID: 5284447. MD is an automatic process for predicting interactions of ligands with their targets, and it was carried out using AutoDock 4.2 software package.

At first, all pdb files were improved by adding hydrogens, using Autodock builder module, and Gasteiger charges were added to the systems. The protein was kept rigid, while the ligand was set to rotate freely. Targeted or focused docking was performed on Sudlow's binding site I. Grid center was -29.436, -17.122 and -0.007. Grid box size was set at  $60 \times 60 \times 60$  °A, and at a spacing parameter of 0.375 °A, to allow the ligand to rotate freely. 200 docking runs were performed using Lamarckian genetic algorithm, consisting of maximum 25,000,000 energy evaluation and 27,000 maximum number of generations.

#### Results and discussion

#### Absorption spectra

Changes in structure and formation of complexes can be studied through absorption spectra. Interaction between two species can affect excited states of chromophores and alter absorption spectra. Fig. 1-a shows that aromatic amino acid residues in HSA gave rise to two absorption peaks at 226 and 278 nm. NA absorption spectrum

features three peaks at 290, 303 and 319 nm (Fig. 1-b). Addition of NA to HSA dramatically increased intensity of HSA peaks (Fig. 1-c). It can be assumed that interaction with NA and formation of HSA-NA complex led to changes in structure and microenvironment of HSA [42, 43].

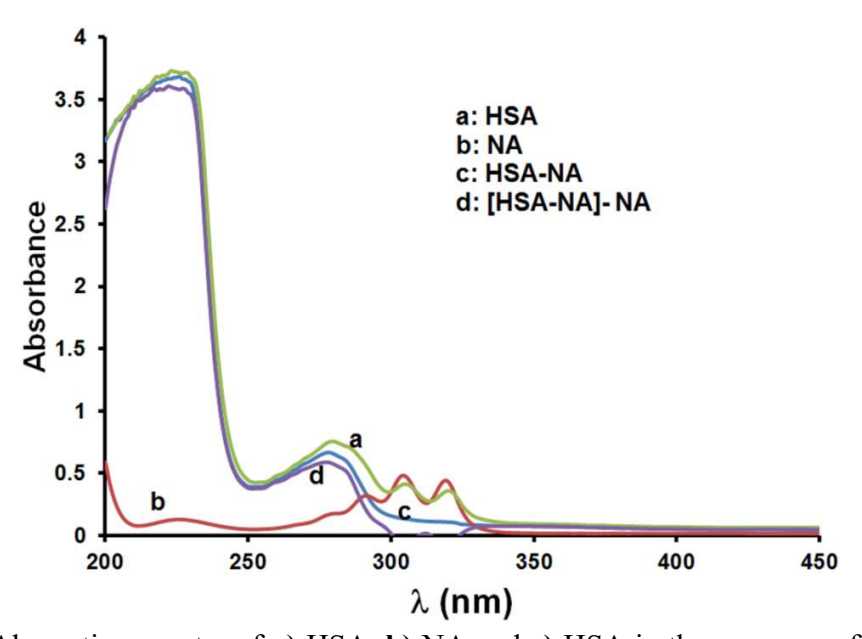


**Figure 1:** Absorption spectra of **a)** HSA, **b)** NA and **c)** HSA in the presence of NA (HSA-NA) and **d)** difference absorption spectrum between HSA-NA and NA. (T = 298 K, pH = 7.4, [HSA] =  $3.0 \times 10^{-5}$  and [NA] =  $3.0 \times 10^{-5}$  mol/L<sup>-1</sup>).

Binding constant of interaction between HSA and NA can be obtained from absorption spectra. For this purpose, interaction between HSA and NA is assumed to be 1:1, forming a single complex. Additionally, behaviors of binding sites are considered independent, and all species follows Beer's law. In addition, a wavelength where molar absorptivities of HSA and HSA-NA are different was selected. According to the report by [44], binding constant of HSA-NA can be calculated using Eq. (1) [44, 45]:

$$\frac{b}{\Delta A} = \frac{1}{S_t K_b \Delta \varepsilon_{11}[L]} + \frac{1}{S_t \Delta \varepsilon_{11}} \tag{1}$$

where  $S_t$  is total concentration of HSA,  $K_b$  is binding constant, b is light path length (1 cm) and [L] is concentration of uncomplexed NA.  $\Delta \epsilon_{11}$  is defined as  $\epsilon_{11}$ - $\epsilon_{HSA}$ - $\epsilon_{NA}$ , where  $\epsilon_{11}$  is molar absorptivity of the complex, and  $\epsilon_{HSA}$  and  $\epsilon_{NA}$  are molar absorptivities of HSA and NA, respectively.  $\Delta A$  is defined as A-A<sub>0</sub>, where A and A<sub>0</sub> are absorbance of HSA solution, in the presence and absence of NA, respectively. Based on Eq. (1), the relationship between  $1/\Delta A$  and 1/[L] is linear. By drawing

corresponding curve and calculating intercept and slope, binding constant can be obtained from eq. (2) [45, 44].

$$K_b = \frac{Intercept}{Slope} \tag{2}$$

Absorption spectra of HAS, in the absence and presence of NA, at different concentrations, were recorded at 20, 30, 35 and 40 °C (Fig. 2- insets). Plots of 1/(A - A0) versus 1/[L] were drawn, where A<sub>0</sub> is initial absorbance of free HAS, at 278 nm, and A is absorbance in the presence of various concentrations of NA. As described above, values of binding constants (K<sub>b</sub>) from HSA-NA in different temperatures were obtained from the ratio of intercept to slope, by assuming one binding site on HSA.

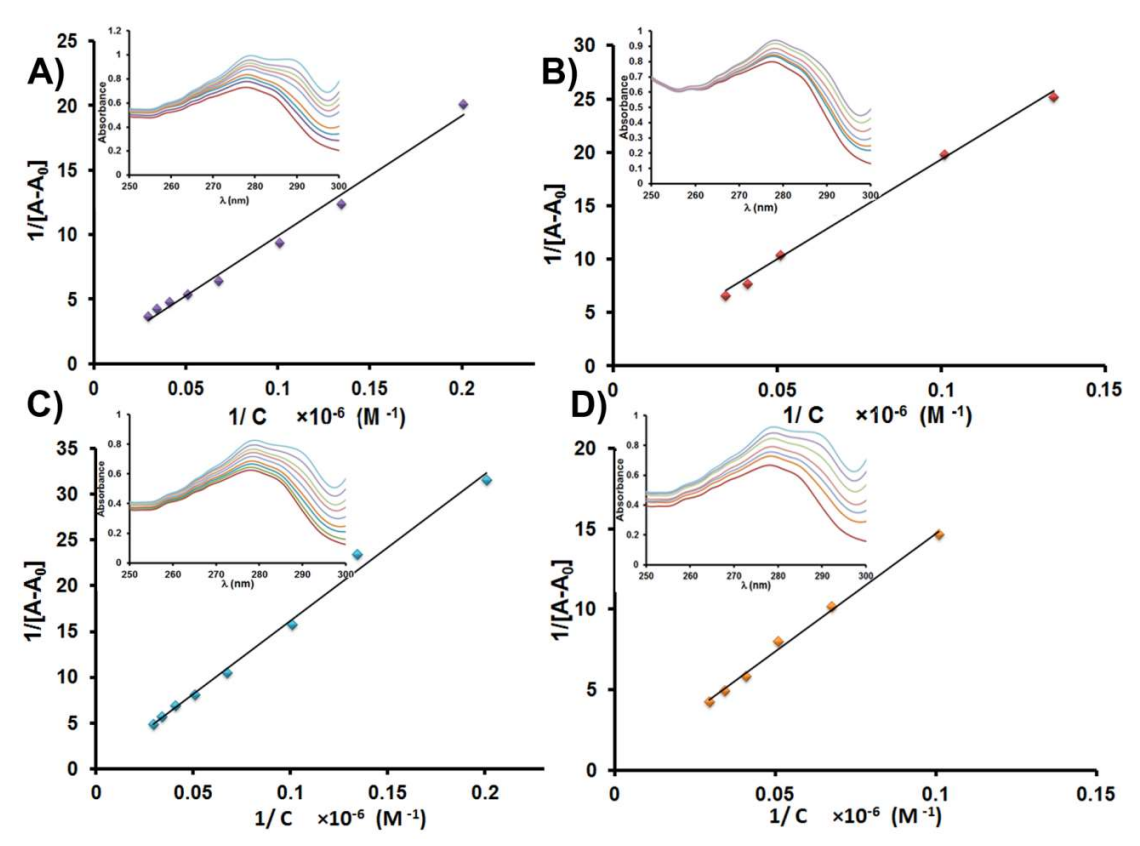


**Figure 2:** Plots of  $1/(A - A_0) vs.$  1/[NA] for determination of  $K_b$  at **A)** 298; **B)** 303; **C)** 308 and **D)** 313 K. Insets: corresponding absorption spectra ([HAS] =  $1.5 \times 10^{-5}$ , [NA] =  $2.5 \times 10^{-6}$  -  $3.4 \times 10^{-5}$ , phosphate buffer pH = 7.4).

Basic non-covalent interaction between small molecules and macromolecules includes Van der Waals force, hydrogen bond, hydrophobic force and electrostatic interactions. To investigate forces between NA and HSA, the relationship between binding constant and temperature was used to analyze thermodynamic parameters and characterize interactions in HSA-NA complex [46, 43]. Main factors for

determining binding mode are enthalpy change ( $\Delta H$ ), entropy change ( $\Delta S$ ) and free energy change ( $\Delta G$ ). If  $\Delta H$  changes are small over studied temperature range, then it can be assumed constant. Subsequently, Van't Hoff Equation (3) can be used for calculating  $\Delta H$  and  $\Delta S$  as follows [46, 43]:

$$lnK_b = -\frac{\Delta H}{RT} + \frac{\Delta S}{R} \tag{3}$$

where R is gas constant and T is absolute temperature (K). Fig. 3 displays the plot of  $lnK_b$  vs. 1/T.  $\Delta H$  and  $\Delta S$  were calculated from slope and intercept of linear plot (Table 1).

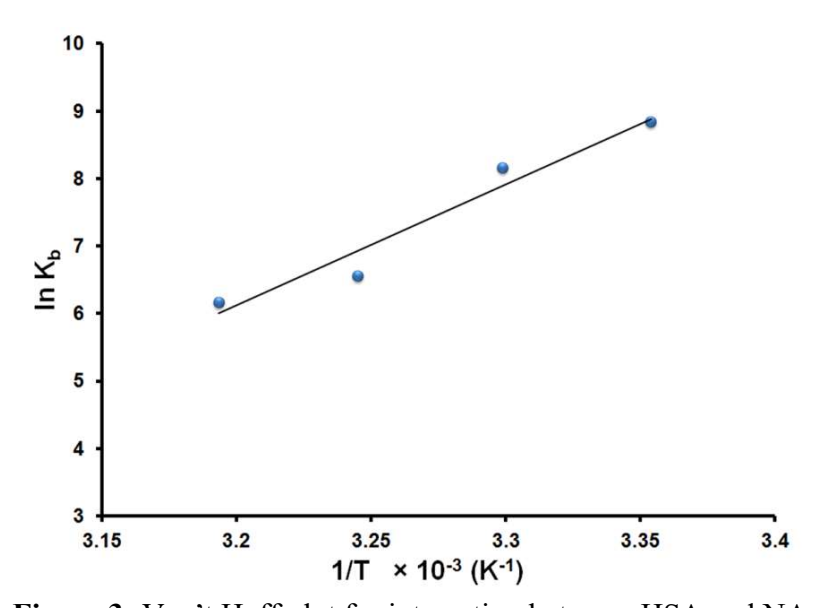


Figure 3: Van't Hoff plot for interaction between HSA and NA.

Gibbs free energy changes in different temperatures were calculated from the following relationship:

$$\Delta G = \Delta H - T\Delta S = -RT \ln K_{\rm b} \tag{4}$$

Results are collected in Table 1. As shown, negative value for free energy change illustrates that binding process between HSA and NA is spontaneous. The relationship between  $\Delta H$  and  $\Delta S$ , with the kind of interaction forces between two molecules, has been previously demonstrated by [47]. Positive  $\Delta H$  and  $\Delta S$  demonstrates hydrophobic interaction. Negative values reflect Van der Waals force or hydrogen bond formation, while  $\Delta H$ <0 and  $\Delta S$ >0 indicate electrostatic force [47]. Accordingly, negative values for obtained  $\Delta H$  and  $\Delta S$  values for interaction between HSA and NA reveal that major forces between these molecules are Van der Waals interactions or hydrogen bonds. Therefore, interaction between HSA and NA involves reduction of  $\Delta H$ ,  $\Delta G$  and  $\Delta S$ , which is mainly driven by enthalpy.

**Table 1:** Binding constants and thermodynamic parameters for the interaction between HSA and NA at various temperatures.

pН	T (K)	Kb	ΔG (kJ/mol)	ΔH (kJ/mol)	ΔS (J/mol/K)
7.4	298	$6.86 \times 10^{3}$	-21.9	-149.2	-426.7
	303	$3.50 \times 10^{3}$	-20.6		
	308	$7.00 \times 10^{2}$	-16.8		
	313	$4.77 \times 10^{2}$	-16.1		

## Electrochemical study

Electroanalysis methods are simple and fast methods, including various techniques that can be divided into interfacial and volume probing techniques. On the other hand, these methods comprise static (potentiometry) and dynamic techniques (controlled potential and controlled current). Cyclic voltammetry is a widely used method that measures current, while working electrode's potential varies in a linear cycle of increase and decrease. In this technique, mass transfer of an electroactive species into the electrode surface is restricted to diffusion, by using a supporting electrolyte, and operating in a quiescent solution (without stirring) [48].

NA is an electroactive compound that can be oxidized on the electrode surface. Fig. 4-a displays CV from a  $1.4 \times 10^{-5}$  mol/L<sup>-1</sup> NA solution in potential range from 0.5 to 1.2 V.

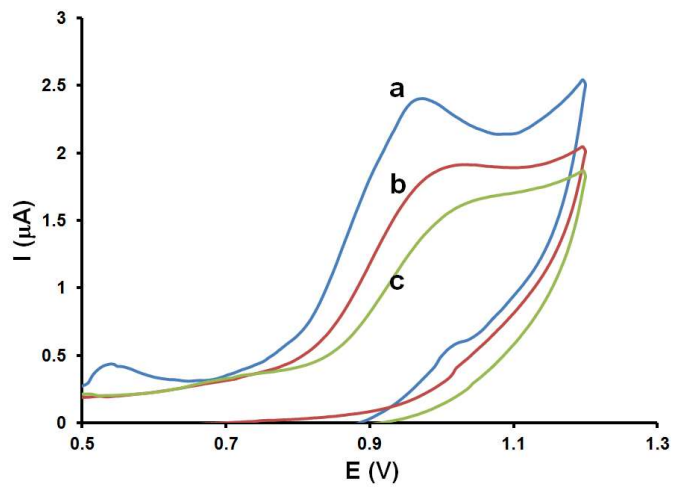


**Figure 4:** CV from **a)**  $1.4 \times 10^{-4}$  mol/L<sup>-1</sup> NA; in the presence of **b)**  $2.0 \times 10^{-6}$  mol/L<sup>-1</sup> HSA and **c)**  $4.0 \times 10^{-6}$  mol/L<sup>-1</sup> HSA (pH = 7.4, scan rate =  $100 \text{ mV/s}^{-1}$ ).

An oxidation peak appears at 0.95 V, with no observed reduction peak, indicating that oxidation of NA on glassy carbon electrode is irreversible. To study the nature of electron transfer process, the effect of potential scan rate on oxidation current of NA was investigated. Results showed that an increase in the scan rate led to higher oxidation currents. Linear plot of oxidation current against square root of scan rate (30–110 mV/s) indicated that mass transfer is controlled by diffusion.

To investigate the interaction between HSA and NA, CV of NA in the presence of  $2.0 \times 10^{-6}$  and  $4.0 \times 10^{-6}$  mol/L<sup>-1</sup> HSA were recorded. Fig. 4-b,c shows that, in the presence of HSA, a significant decrease at peak currents was observed. Additionally, peak potentials have shifted to more positive values (more over voltage).

Positive shifts of oxidation potential indicate that oxidation of NA's surface in the presence of HSA is more difficult. In other words, HSA-NA complex requires more energy to undergo oxidation reaction on the electrode [49]. On the other hand, interaction of the electroactive compound with a large molecular weight biomolecule would cause a significant decrease in diffusion coefficient [49, 50]. Therefore, decreases in peak current may be due to interaction of NA with HAS, which can change parameters of oxidation process.

Variations in oxidation currents, in the presence and absence of HAS, can be used to study the interaction mechanism between HSA and NA, and to estimate binding number and constant. According to the provided procedure, binding number (m) and constant (K<sub>b</sub>) are calculated from Eq. (5) [37]:

$$log\left[\frac{\Delta I}{\Delta I_{max} - \Delta I}\right] = mlogK_b + mlog[NA]$$
 (5)

where  $\Delta I = I_0$ -I, and  $I_0$  and I indicate oxidation peak current of NA, in the absence and presence of HAS;  $\Delta I_{max}$  represents maximum change at peak current; and [NA] is its concentration. From the slope and intercept of linear relation between  $log[\Delta I/\Delta I_{max}-\Delta I]$  vs. log[NA], binding number and constant for HSA-NA can be calculated [34, 37, 51]. Fig. 5 shows that plot's slope is nearly unity (0.754), indicating a 1:1 stoichiometric ratio for HSA-NA [50]. In addition,  $K_b$  was calculated from intercept as  $7.4\times10^3$ , which is close to previous value obtained via spectroscopic method.

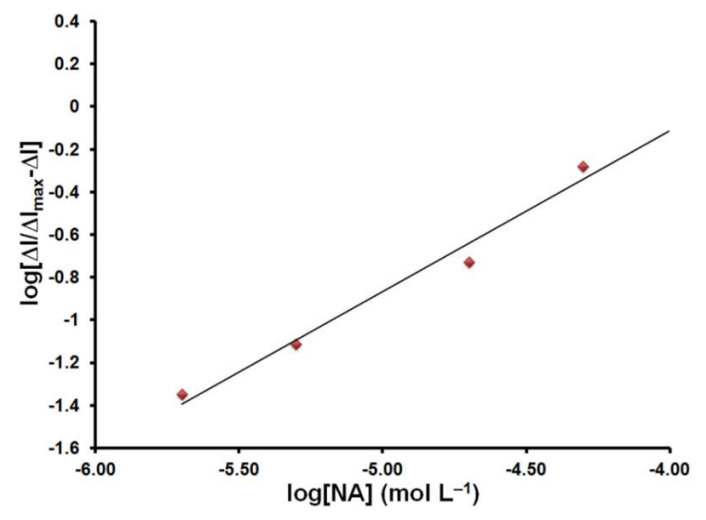


**Figure 5:** Relationship  $\log[\Delta I/\Delta I_{max}-\Delta I]$  with  $\log[NA]$ .

Chronoamperometry is an electrochemical method in which a potential step is applied to the working electrode, and current is measured as function of time. If the current in electrode reaction is diffusion-limited, then the current after application of potential step will obey Cottrell equation as follows [48]:

$$i_t = \frac{nFAD^{1/2}C}{\pi^{1/2}t^{1/2}} \tag{6}$$

where  $i_t$  is current, n is number of electrons, F is Faraday constant, A is the electrode's surface area (cm²), C is concentration of electroactive species (mol/cm³), C is time and C indicates diffusion coefficient of electroactive species (cm²/s⁻¹). Value of C is determined by plotting C against C Chronoamperograms of C NA, in the absence and presence of HAS, at C 10⁻⁶ and C 10⁻⁶ mol/C were recorded by applying a potential step at C 12 V. Fig. 6 shows that current is higher in albumin absence than in its presence, maybe because it hinders NA's ability to diffuse toward the electrode's surface [37, 50]. Diffusion coefficient calculated for electroactive species using Cottrell equation was C 10⁻⁶ mol/C without HSA, and C 10⁻⁶ and C 10⁻⁶ mol/C HSA concentrations, respectively, which aligns with observations.

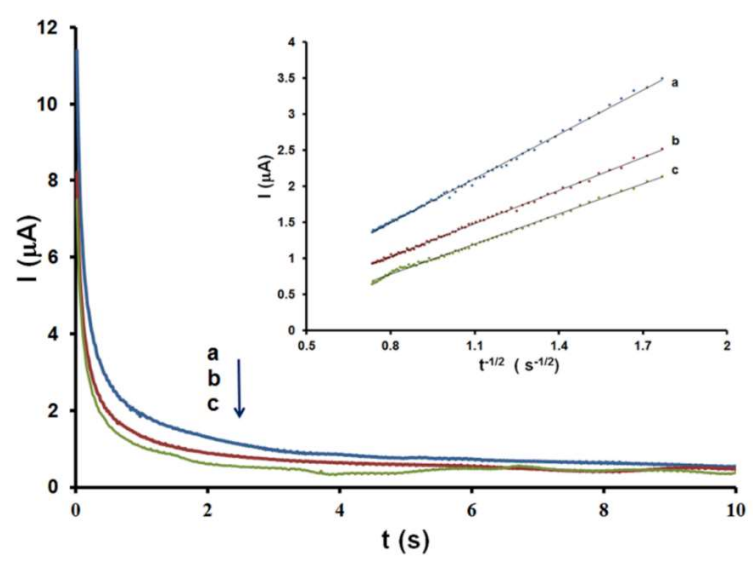


**Figure 6**: Chronoamperograms of **a)**  $1.4 \times 10^{-4}$  mol/L<sup>-1</sup> NA; with **b)**  $2.0 \times 10^{-6}$  mol/L<sup>-1</sup> HSA and **c)**  $4.0 \times 10^{-6}$  mol/L<sup>-1</sup> HSA (pH = 7.4, potential step = 1.2 V). Inset: Cottrell Plots.

# Molecular docking studies

MD was performed to investigate the interaction between protein and ligand, and its results are presented in Table 2. Lowest binding energy was predicted to be -8.78 kcal/mol, which indicates strong binding affinity to HSA. Sudlow site I is known to accommodate a wide range of drugs, and it plays a critical role in

drug delivery, due to its high binding affinity. Fig. 7 shows that NA ligand has three H bonds with residues of Glu292, Ala291 and Arg218, and it has twelve Van an der Waals with residues of Glu188, His288, Tyr452, Tyr150, Glu153, Ser287, Val241, Ile290, Leu219, Trp214, Arg222 and Lys195. The other bonds are Pi double bonds with an aromatic plane.

Docking results	Natamycin
Cluster rank	2
Number in cluster	83
$K_{i}$	366.86 nM
vdW + Hbond + desolv energy (kcal/mol) (1)	-8.95
Electrostatic energy (kcal/mol) (2)	-2.81
Torsional free energy (kcal/mol) (3)	2.98
Lowest binding energy (kcal/mol) (1+2+3)	-8 78

**Table 2:** Autodock results between HSA and NA.

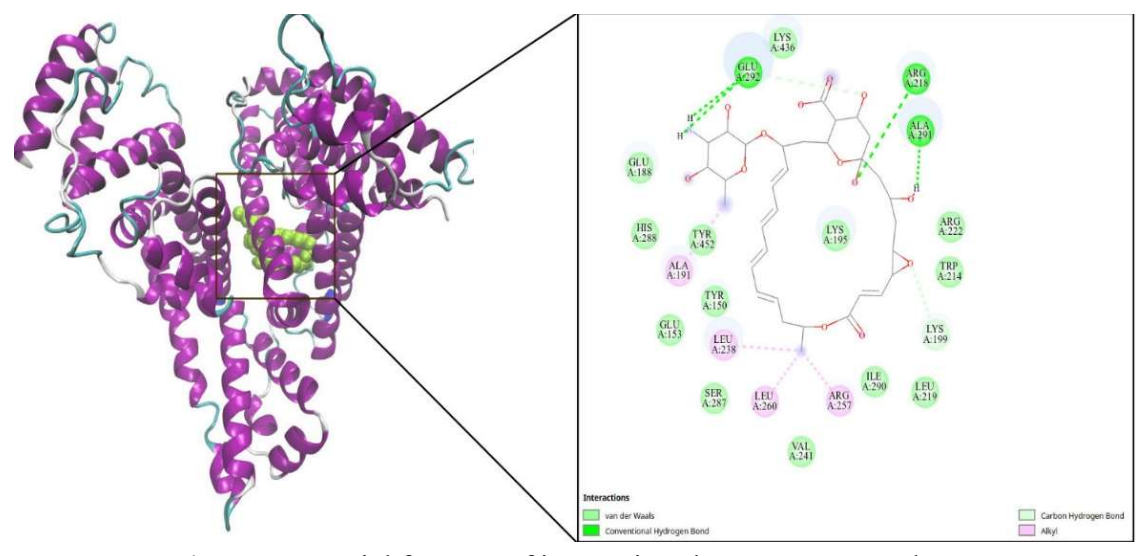


**Figure 7:** Special features of interactions between HSA and NA.

#### Conclusion

Interaction between human serum albumin and Natamycin was studied using UV-Vis spectroscopy, electrochemical techniques and MD. Results showed that the interaction of HSA with NA caused an increase in HAS's absorption peak, which led to changes in its structure and microenvironment. Additionally, this interaction caused a decrease electrochemical activity of NA on glassy carbon electrode surface. Calculated thermodynamic parameters showed that binding reaction of NA with HSA is spontaneous, and the major force between these molecules is Van der Waals interactions or hydrogen bonds. Results of the interaction between NA and HSA

with MD support the proposed binding interaction. These findings provide valuable insights into binding mechanism and thermodynamic properties of HSA-NA complex, contributing to a better understanding of pharmacokinetics of NA and its potential applications in drug delivery systems.

## **Acknowledgments**

The authors gratefully acknowledge Islamic Azad University, Falavarjan Branch research council, for supporting this work.

#### Data availability statement

All data related to this study are available within the manuscript.

## **Funding declaration**

This study did not receive any funding.

#### **Conflict of interest**

The authors declare the absence of any pertinent financial or non-financial interests that could potentially influence the content disclosed in this manuscript.

#### **Authors' contributions**

**Masoud Fouladgar:** methodology, investigation, collected the data, conceived and designed the analysis, writing original draft, review and editing. **Maryam Khademi Dehkordi:** Molecular docking, writing original draft.

#### **Abbreviations**

CV: cyclic voltammogram HSA: human serum albumin

**K**<sub>b</sub>: binding constant **MD**: molecular docking

**NA**: Natamycin

# **Symbols definition**

ΔG: free energy changeΔH: enthalpy changeΔS: entropy change

#### References

1. Szomek M, Akkerman V, Lauritsen L et al. Ergosterol promotes aggregation of natamycin in the yeast plasma membrane. Biochim Biophys Acta (BBA) - Biomemb. 2024;1866(7):184350. https://doi.org/10.1016/j.bbamem.2024.184350

- 2. Jagus RJ, Gerschenson LN, Ollé RCP. Chapter 49 Combinational Approaches for Antimicrobial Packaging: Natamycin and Nisin, In: Barros-Velázquez J (ed), Antimicrobial Food Packaging, Academic Press, San Diego, 2016. https://doi.org/10.1016/B978-0-12-800723-5.00049-8
- 3. Patil A, Lakhani P, Majumdar S. Current perspectives on natamycin in ocular fungal infections. J Drug Deliv Sci Technol. 2017;41:206-212. https://doi.org/10.1016/j.jddst.2017.07.015
- 4. Delves-Broughton J, Weber G. Nisin, natamycin and other commercial fermentates used in food biopreservation. In: Lacroix C (ed), Protective Cultures, Antimicrobial Metabolites and Bacteriophages for Food and Beverage Biopreservation, Woodhead Publishing, 2011. https://doi.org/10.1533/9780857090522.1.63
- 5. EFSA. Scientific Opinion on the use of natamycin (E 235) as a food additive. EFSA J. 2009;7:1412. https://doi.org/10.2903/j.efsa.2009.1412
- 6. Kerridge D. Polyene Macrolide Antibiotics. In: Vanden Bossche H, Mackenzie DWR, Cauwenbergh G (eds), Aspergillus and Aspergillosis, Springer US, Boston, MA, 1988. https://doi.org/10.1007/978-1-4899-3505-2 14
- 7. Lin EX, Miao F, Tao TL et al. Application and research progress of natamycin in fungal keratitis. Chin J New Dru. 2024; 33(11):1115-1120.
- 8. Tian X, Zhan L, Long X et al. Multifunctional natamycin modified chondroitin sulfate eye drops with anti-inflammatory, antifungal and tissue repair functions possess therapeutic effects on fungal keratitis in mice. Intern J Bio Macromol. 2024;279:135290. https://doi.org/10.1016/j.ijbiomac.2024.135290
- 9. Haq HU, Altunay N, Tuzen M et al. Quality control of cheese samples for the presence of natamycin preservative A natural deep eutectic solvent (NADES) based extraction coupled with HPLC. J Food Compos Analy. 2024;129:106101. https://doi.org/10.1016/j.jfca.2024.106101
- 10. EFSA. Scientific support for preparing an EU position in the 50th Session of the Codex Committee on Pesticide Residues. EFSA J. 2018;16(7):5306. https://doi.org/10.2903/j.efsa.2018.5306
- 11. Administration UFaD (2024) Food Additive Status List. https://www.fda.gov/food/food-additives-petitions/food-additive-status-list#ftnN. Accessed 22 September 2024
- 12. Arques S. Human serum albumin in cardiovascular diseases. Eur J Inter Med. 2018;52:8-12. https://doi.org/10.1016/j.ejim.2018.04.014
- 13. Zheng L, Zeng Z, Zhao Y et al. HSADab: A comprehensive database for human serum albumin. Intern J Bio Macromol. 2024;277:134289. https://doi.org/10.1016/j.ijbiomac.2024.134289

- 14. Ullah A, Shin G, Lim SI. Human serum albumin binders: A piggyback ride for long-acting therapeutics. Drug Discov Tod. 2023;28(10):103738. https://doi.org/10.1016/j.drudis.2023.103738
- 15. Tabachnick M, Giorgio NA. Thyroxine-protein interactions: II. The binding of thyroxine and its analogues to human serum albumin. Arch Biochem Biophys. 1964;105(3):563-569. https://doi.org/10.1016/0003-9861(64)90051-7
- 16. Wang Y, Yu H, Shi X et al. Structural Mechanism of Ring-opening Reaction of Glucose by Human Serum Albumin. J Biolog Chem. 2013;288(22):15980-15987. https://doi.org/10.1074/jbc.M113.467027
- 17. Yang F, Bian C, Zhu L et al. Effect of human serum albumin on drug metabolism: Structural evidence of esterase activity of human serum albumin. J Struc Bio. 2007;157(2):348-355. https://doi.org/10.1016/j.jsb.2006.08.015
- 18. Guo J-L, Liu G-Y, Wang R-Y et al. Synthesis and Structure Elucidation of Two Essential Metal Complexes: In-Vitro Studies of Their BSA/HSA-Binding Properties, Docking Simulations, and Anticancer Activities. Molecules. 2022;27(6):1886. https://doi.org/10.3390/molecules27061886
- 19. Richter-Bisson ZW, Nie HY, Hedberg YS. Serum protein albumin and chromium: Mechanistic insights into the interaction between ions, nanoparticles, and protein. Intern J Biol Macromol. 2024;278:134845. https://doi.org/10.1016/j.ijbiomac.2024.134845
- 20. Shafaei P, Rastegari AA, Fouladgar M et al. Insight into the binding of alphalinolenic acid (ALA) on human serum albumin using spectroscopic and molecular dynamics (MD) studies. Proc Biochem. 2022;122:95-104. https://doi.org/10.1016/j.procbio.2022.09.022
- 21. Peymaneh S, Rastegari AA, Fouladgar M. Investigation of the Several Aspects of Interaction between Human Serum Albumin and Oleic Acid by Molecular Dynamic Simulation Approaches and Spectroscopic Methods. Biochem (Moscow), Suppl Ser B: Biomed Chem. 2024;18(1):91-102. https://doi.org/10.1134/S1990750823600346
- 22. Xu X, Hu J, Xue H et al. Applications of human and bovine serum albumins in biomedical engineering: A review. Intern J BioMacromol. 2023;253:126914. https://doi.org/10.1016/j.ijbiomac.2023.126914
- 23. Maciążek-Jurczyk M, Szkudlarek A, Chudzik M et al. Alteration of human serum albumin binding properties induced by modifications: A review. Spectrochim Acta Part A: Mol Biomo Spectrosc. 2018;188:675-683. https://doi.org/10.1016/j.saa.2017.05.023
- 24. Wang Q, Chang KL, Fan JW et al. Construction of a human serum albumin site II-targeting supramolecular fluorescent probe for cell imaging and drug delivery. J Mol Struc. 2024;1312:138503. https://doi.org/10.1016/j.molstruc.2024.138503

- 25. Peyrin E, Guillaume YC, Guinchard C. Characterization of Solute Binding at Human Serum Albumin Site II and its Geometry Using a Biochromatographic Approach. Biophys J. 1999;77(3):1206-1212. https://doi.org/10.1016/S0006-3495(99)76972-9
- 26. Sudlow G, Birkett DJ, Wade DN. The characterization of two specific drug binding sites on human serum albumin. Mol Pharmacol. 1975;11(6):824-832.
- 27. Ahmad Hidayat AF, Mohamad SB, Tayyab S et al. Molecular interaction of a protease inhibitor, leupeptin, with human serum albumin: Insights from calorimetry, spectroscopy, microscopy, and computational approaches. J Mol Struc. 2025;1321:139670. https://doi.org/10.1016/j.molstruc.2024.139670
- 28. Rupreo V, Tissopi R, Baruah K et al. Multispectroscopic and Theoretical Investigation on the Binding Interaction of a Neurodegenerative Drug, Lobeline with Human Serum Albumin: Perturbation in Protein Conformation and Hydrophobic-Hydrophilic Surface. Mol Pharm. 2024;21(8):4169-4182. https://doi.org/10.1021/acs.molpharmaceut.4c00651
- 29. Maciel TMS, J Nascimento JSI, da Silva LN et al. Biophysical studies of human serum albumin with cocaine and cocaethylene: Understanding the drugprotein interaction in simulated physiological conditions. J Mol Liq. 2024;410:125570. https://doi.org/10.1016/j.molliq.2024.125570
- 30. Tong WH, Wang SQ, Chen GY et al. Characterization of the structural and molecular interactions of Ferulic acid ethyl ester with human serum albumin and Lysozyme through multi-methods. Spectrochim Acta Part A: Mol Biomol Spectrosc. 2024;320:124549. https://doi.org/10.1016/j.saa.2024.124549
- 31. Wulf J, Lewit N, Akter S et al. Evaluating binding and interaction of selected pesticides with serum albumin proteins by Raman, 1H NMR, mass spectrometry and molecular dynamics simulation. J Biomol Struc Dynam. 2025; 45(5):2571-2584. https://doi.org/10.1080/07391102.2024.2302344
- 32. Aiello F, Uccello-Barretta G, Picchi C et al. NMR Investigation of the Interaction of Three Non-Steroidal Anti-Inflammatory Drugs with Human Serum Albumin. Molecules. 2022;27(19):6647. https://doi.org/10.3390/molecules27196647
- 33. Wang B, Qin Q, Chang M et al. Molecular interaction study of flavonoids with human serum albumin using native mass spectrometry and molecular modeling. Analyt Bioanalyt Chem. 2018;410(3):827-837. https://doi.org/10.1007/s00216-017-0564-7
- 34. Sun W, Jiao K, Wang X et al. Electrochemical studies of the reaction between albumin and amaranth and its analytical application. J Electroanalyt Chem. 2005;578(1):37-43. https://doi.org/10.1016/j.jelechem.2004.11.042

- 35. Keciba A, Bakirhan NK, Gündüz MG et al. Electrochemical and Theoretical Investigations on the Binding of Anticancer Drug Olaparib to Human Serum Albumin. J Electrochem Soc. 2024;171(6):066507. https://doi.org/10.1149/1945-7111/ad590d
- 36. Bakirhan NK, Brahmi M, Gündüz MG et al. Experimental and computational perspectives on the interaction of nerve agent VX metabolite ethyl methylphosphonic acid with human serum albumin. Microchem J. 2024;205:111406. https://doi.org/10.1016/j.microc.2024.111406
- 37. Chenguiti F, Bakirhan NK, Gozelle M et al. Enzalutamide-human serum albumin interaction: Electrochemical exploration of complex formation and binding parameters. Microchem J 2024;201:110760. https://doi.org/10.1016/j.microc.2024.110760
- 38. Li Z, Chen L, Chen R et al. The study of interaction between human serum albumin and alternaria toxins using multi-spectroscopy, molecular docking and molecular dynamic. J Mol Struc. 2024;1315:138774. https://doi.org/10.1016/j.molstruc.2024.138774
- 39. Shafaei P, Rastegari AA, Fouladgar M et al. Investigation of structural changes in human serum albumin after binding with elaidic acid. J Mol Struc. 2023;1272:134134. https://doi.org/10.1016/j.molstruc.2022.134134
- 40. Xu L, Huang W, Lin Y et al. Interaction and binding mechanism of anticancer echinacoside phenylethanoid glycoside against hepatocellular carcinoma with subdomains of human serum albumin. Arab J Chem. 2024;17(9):105869. https://doi.org/10.1016/j.arabjc.2024.105869
- 41. Khan S, Naeem A. Bovine serum albumin prevents human hemoglobin aggregation and retains its chaperone-like activity. J Biomole Struc Dyn. 2024;42(1):346-361. https://doi.org/10.1080/07391102.2023.2192802
- 42. Azimirad M, Javaheri-Ghezeldizaj F, Yekta R et al. Mechanistic and kinetic aspects of Natamycin interaction with serum albumin using spectroscopic and molecular docking methods. Arab J Chem. 2023;16(9):105043. https://doi.org/10.1016/j.arabjc.2023.105043
- 43. Xu H, Yao N, Xu H et al. Characterization of the Interaction between Eupatorin and Bovine Serum Albumin by Spectroscopic and Molecular Modeling Methods. Intern J Mol Sci. 2013;14(7):14185-14203. 10.3390/ijms140714185
- 44. Bourassa P, Dubeau S, Maharvi GM et al. Binding of antitumor tamoxifen and its metabolites 4-hydroxytamoxifen and endoxifen to human serum albumin. Biochimie. 2011;93(7):1089-1101. https://doi.org/10.1016/j.biochi.2011.03.006

- Mehraban MH, Yousefi R, Taheri-Kafrani A et al. Binding study of novel anti-diabetic pyrimidine fused heterocycles to β-lactoglobulin as a carrier protein.
  Coll Surf B: Biointerf. 2013;112:374-379. https://doi.org/10.1016/j.colsurfb.2013.08.013
- 46. Zhang W, Wang F, Xiong X et al. Spectroscopic and molecular docking studies on the interaction of dimetridazole with human serum albumin. J Chil Chem Soc. 2013;58(2):1717-1721. http://dx.doi.org/10.4067/S0717-97072013000200016
- 47. Ross PD, Subramanian S. Thermodynamics of protein association reactions: forces contributing to stability. Biochemistry. 1981;20(11):3096-3102. https://doi.org/10.1021/bi00514a017
- 48 Bard AJ, R.Faulkner L. Electrochemical Methods Fundamentals and Applications. 2nd edn. John Wiley & Sons. 2001.
- 49. Wang S, Peng T, Yang CF. Electrochemical determination of interaction parameters for DNA and mitoxantrone in an irreversible redox process. Biophys Chem. 2003;104(1):239-248. https://doi.org/10.1016/S0301-4622(02)00371-X
- 50. Ender B, Mustafa M. Electrochemical and Molecular Docking Studies on the Interactions of (Z)-1-[(2,4-dimethoxyphenylamino)methylene]naphthalen-2(1H)-one with Calf Thymus DNA, HSA and BSA Biomolecules. Russ J Electrochem. 2023;59(11):969-980. https://doi.org/10.1134/S1023193523110058
- 51. Sun W, Han J, Jiao K et al. Studies on the interaction of protein with acid chrome blue K by electrochemical method and its analytical application. Bioelectrochemistry. 2006;68(1):60-66. https://doi.org/10.1016/j.bioelechem.2005.03.007